CRYSTAL GROWTH & DESIGN
2008
VOL. 8, NO. 6
2019–2023

Morphology Evolution of Sb_2S_3 under Hydrothermal Conditions: Flowerlike Structure to Nanorods

Jyotiranjan Ota,[†] Poulomi Roy,[†] Suneel Kumar Srivastava,*[,†] Bijan Bihari Nayak,[‡] and Arvind Kumar Saxena[§]

Inorganic Materials and Nanocomposites Laboratory, Department of Chemistry, Indian Institute of Technology, Kharagpur-721302, India, Mineralogy Cell, Institute of Minerals and Materials Technology, Bhubaneswar-751013, India, Defense Materials and Stores Research and Development Establishment, Kanpur-208013, India

Received November 17, 2007; Revised Manuscript Received January 18, 2008

ABSTRACT: Nanorods of Sb_2S_3 have been synthesized by a surfactant assisted hydrothermal method. The formation of nanorods through flowerlike morphology with an intermediate straw tide like structure has been depicted by scanning electron microscopy (SEM) study. This type of observation is the first of its kind for this material, and it has been explained on the basis of a two step heterogeneous nucleation−growth mechanism followed by crystal splitting. Raman spectroscopy of the nanorods has been carried out to provide an idea about their purity. An increase in the band gap is observed for Sb_2S_3 with nanorod-type morphology. Photoluminescence (PL) shows no sign of quantum confinement effect, though a large increase in intensity for nanorods has been observed compared to the flowerlike morphology.

Introduction

Recently, inorganic materials with controllable size and various type of unique morphology are being studied due to their novel physical and chemical properties.[1−4] In the process, simulation based studies have interpreted the possible synthesis of different morphologies existing in nature, e.g. zebra stripes, trees, butterfly wings etc.[5] There are also a number of experimental reports on various morphologies like nanorings, cones, dendrites, urchins etc. that take inspiration from naturally occurring structures.[6−9] Such anisotropic growth of the materials is due to their typical crystal structure as well as the extreme reaction conditions they are subjected to. Thus, Sb_2S_3, owing to its characteristic structure, has been synthesized in various interesting morphologies that resemble a number of naturally existing structures. For example, Xie and co-workers prepared Sb_2S_3 with dendrite-type morphology and explained this based on crystallization of amorphous colloidal microspheres.[10] Qian et al. have synthesized Sb_2S_3 in a number of novel morphologies such as radioactive dendrite, prickly sphere, flowerlike structures, featherlike structure etc. by a typical solvothermal method.[11] They discussed this unusual but interesting structure of the material on the basis of anisotropic crystal structure as well as a stepwise nucleation and growth process. The same group has also prepared straw tide like morphologies made out of nanorods in an ethylene diamine complex based solvothermal process and discussed its formation, based on a solid−solution−solid (SSS) mechanism.[12] Recently, microcones of Sb_2S_3 also have been reported, where the spiral bending of the thin films of the material was responsible for this novel structure.[13] In the mean time, there already exist a number of reports toward synthesis of nanorods of Sb_2S_3. So far, various synthetic methods such as hydrothermal,[14] sonochemical,[15] complexing agent assisted,[16] single source decomposition,[17] and polyol assisted routes[18] have been employed to synthesize this material either in rod, ribbon or wire form. Lu and co-workers reported various novel morophologies like dumbbell shape or spheres formed out of ordered aggregation of the nanorods.[19] They proposed that the surfactant (PVP) present in the solution played a key role for the typical attachment of the nanorods and termed it imperfect oriented attachment (IOA). However, till now there has been very little development regarding the synthesis of this material in various possible morphologies and especially the growth of nanomaterials using simple chemical methods is not much studied. Taking into account the technical importance of this material, fabricating it in some typical naturally inspired structures has always been a great interest. Moreover, use of surfactants for controlling the growth of this material is not sufficiently exploited. With this motivation, we tried to design a surfactant assisted reaction and observe the morphology evolution of this interesting material.

The present article describes synthesis of nanorods of Sb_2S_3 via a surfactant assisted hydrothermal route. The essence of this work lies in formation of microflowerlike structures initially and subsequently their transformation into nanorods through a straw tide like intermediate. This hierarchical transformation of novel structures to form nanorods as the final product is the first of its kind. In addition, photoluminescence (PL) is a useful contactless procedure for defect and impurity study of the materials. Nevertheless, to the best of our knowledge, room temperature PL of Sb_2S_3 nanostructures has never been investigated. Hence, in this paper we report the PL properties of Sb_2S_3 nanorods.

Experimental Details

Materials and Characterization. All the reagents were of analytical grade and used without further purification. Antimony trichloride ($SbCl_3$) was obtained from Loba Chemicals, India. Triethanolamine (TEA) was supplied by Merck, India. Sodium dodecyl sulfate (SDS), carbon disulfide (CS_2), TX-100, and ammonia (NH_3) were procured from SRL, India.

Powder XRD of the sample was recorded on a Philips PW-1710 X-ray diffractrometer (40 kV, 20 mA) using Cu Kα radiation (λ = 1.5418 Å) in the range 10−70° at a scanning rate 0.5° min^{-1}. The morphology of the samples was studied by scanning electron microscope (SEM) using JEOL (JSM-5800) at an accelerating voltage 20 kV. A JEOL 2100 transmission electron microscope operating at 200

* Corresponding author. Tel: 91-3222-283334. Fax: 91-3222-255303. E-mail: sunit@chem.iitkgp.ernet.in.
[†] Indian Institute of Technology.
[‡] Institute of Minerals and Materials Technology.
[§] Defense Materials and Stores Research and Development Establishment.

10.1021/cg701133b CCC: $40.75
Published on Web 05/16/2008

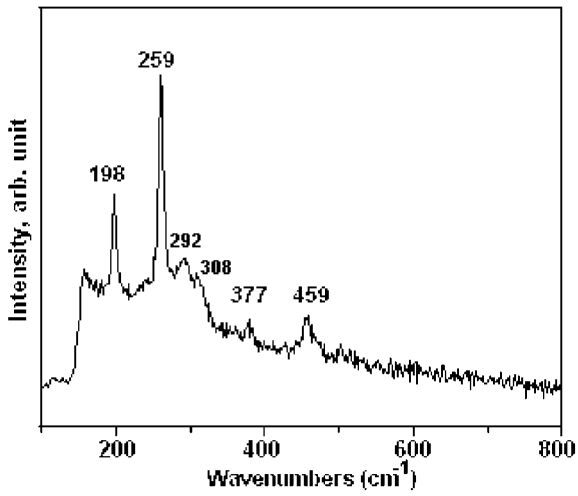

Figure 1. Raman spectrum of the product obtained after 24 h.

kV was used for TEM, HRTEM and SAED analysis of the sample drop casted on carbon-coated Cu grid from dispersion in ethanol. Images were acquired digitally on a Gatan multipole CCD camera. Optical measurement of the sample, dispersed in ethanol, was done on a Perkin-Elmer Lambda 20 UV/vis spectrophotometer. The photoluminescence measurements were performed on a Perkin-Elmer LS55 luminescence spectrophotometer. Raman spectra were collected on a RENISHAW inVia Raman microscope equipped with Ar ion laser of wavelength 514.5 nm.

Synthetic Procedure. In a typical experiment 0.52 g of SDS was added to 30 mL of water followed by 0.6 mL of CS_2 and 0.4 mL of NH_3 (13.6 N). To the resultant solution was added 0.625 g of $SbCl_3$ triturated in TEA, and the mixture was refluxed at 60 °C for 2−3 h. The resultant orange colored solution was poured in to a 55 mL stainless still autoclave lined with Teflon and heated for 12−24 h. The resultant black precipitate was filtered, washed with distilled water followed by ethanol and dried under vacuum for 4 h at 60 °C. Finally the grayish black powder was taken for characterization.

Result and Discussion

The phase analysis of the sample was performed by XRD, and all the peaks in corresponding diffractogram are in accord with orthorhombic phase of Sb_2S_3 (JCPDS: 06-0474). It is also noted that all the major (*hk*0) planes are of relatively higher intensity compared to their reported value. This indicates that the crystal growth is preferably along the (00*l*) direction, which is in agreement with the one dimensional growth of the materials and a first hand observation for possible formation of 1D nanostructures in the product.

In order to further ascertain the quality of the product so obtained, material was characterized by Raman spectroscopy and the corresponding spectrum is displayed in Figure 1. The appearance of the peaks at 198, 259, 292, 308, 377 and 459 cm^{-1} is in good agreement with the Raman spectrum reported by Lopez et al.[20] for Sb_2S_3 inverted opals as well as that for the commercial stibinite. The presence of sharp peaks at 198 and 259 cm^{-1} suggests the formation of well crystalline product. The low intensity peaks at 292 and 308 cm^{-1} can be assigned to the unit SbS_3 pyramid of the material having C_{3v} symmetric modes.[21] The presence of a relatively broad peak at 459 cm^{-1} may be due to the symmetric stretching of the Sb−S−S−Sb bond of Sb_2S_3, which can be accounted on the basis of existing literature.[22] Thus, all the peaks in the Raman spectra of the product obtained at 24 h are successfully assigned to the crystalline form of Sb_2S_3 with no additional peaks for the impurity present in the product.

Extensive electron microscopic studies, especially SEM, have been performed to unfold the morphology of the Sb_2S_3 obtained at different duration of the reaction, and their respective micrographs are shown in Figure 2. Figure 2a refers to the image of final product obtained after 24 h that consists of a one-dimensional nanostructure with diameter in the nanometer range and length of a few microns. No other morphological features of Sb_2S_3 could be observed in this image, suggesting that almost all products obtained as such are in the form of nanorods. In order to study the details of formation mechanism of these nanorods, products obtained at different time duration (12 and 18 h) have also been studied extensively by SEM. The product obtained at 12 h (Figure 2b) mainly consists of some typical flowerlike structures. These structures have nearly 6−8 μm end to end dimensions with three petals and a central nucleus. In addition, some detached petal-like structures with split ends are also observable. When the reaction duration is increased to 18 h, some straw tide like structure could be seen in the product as can be observed in Figure 2c. These structures are very unique with nanorods emerging out of a central nucleus. It seems as if the petals have been broken down into nanorods with one end of each attached to the nucleus of the microflowers, and well dispersed nanorods are the major product for reaction duration of 24 h.

On the basis of the SEM analysis, it is clear that initially flowerlike morphologies are formed and these are subsequently transformed into nanorods through a straw tide like structure. On the basis of the above observations and taking into consideration the typical crystal structure of the material, a growth mechanism for the formation of these nanorods can be proposed. Previously, a number of works have described the formation of novel morphologies of Sb_2S_3 by means of stepwise heterogeneous nucleation and growth as well as anisotropy.[11,12] Based on the mechanism proposed earlier and our present observations, we put forth a two step mechanism, where the first step leads to the crystal growth and the second step is crystal breaking. Herein, the formation of flowerlike morphology is based on heterogeneous nucleation and second breaking process or crystal splitting is due to typical layered structure of Sb_2S_3. In this process, amorphous Sb_2S_3 nanoparticles formed during the refluxing conditions are stabilized by the surfactant molecules and prevent the aggregation of the particles owing to presence of their long hydrocarbon chain. Subsequently, these nanoparticles are subjected to a heterogeneous nucleation process resulting in flowerlike structures. During this heterogeneous nucleation process, growth of Sb_2S_3 nanoparticles occurs along the specific energetically favorable sites that are likely to be promoted by the surfactant molecules. In addition, the typical polymer chain like anisotropy of the crystal structure of Sb_2S_3 is also pivotal for this type of growth. Oswald ripening process follows this, making the crystals grow into unique flowerlike structures. With increase in reaction duration, the petals of these flowerlike structures break into rods with their one end attached to the starting nucleus, forming a straw tide like structure. This type of breaking or crystal splitting occurs due to the favorable crystal structure of Sb_2S_3, which usually crystallizes in an orthorhombic structure with typical chain like $(Sb_4S_6)_n$ moieties running parallel to the 001 axis that contains two types of Sb and three types of S atoms.[16] Out of the three types of sulfur atoms, two are formally trivalent and one is divalent. Within the chain, the divalent sulfur and one trivalent sulfur are connected to antimony by strong covalent bonds. However, the third sulfur is connected to the antimony of the second parallel running chain by weaker van der Waals bonds

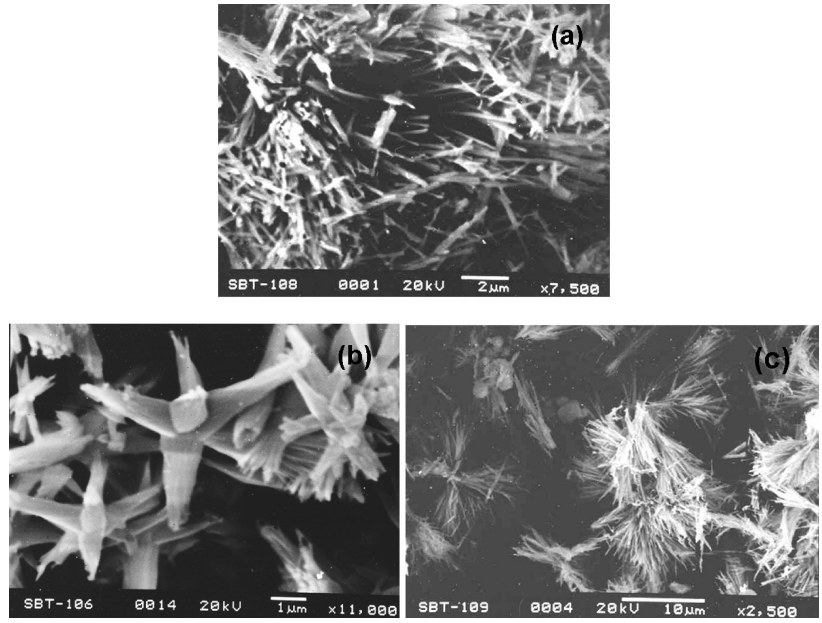

Figure 2. SEM image of the product obtained after (a) 24 h, (b) 12 h, (c) 18 h of reaction duration showing nanorod, flowerlike and straw tide like morphology respectively.

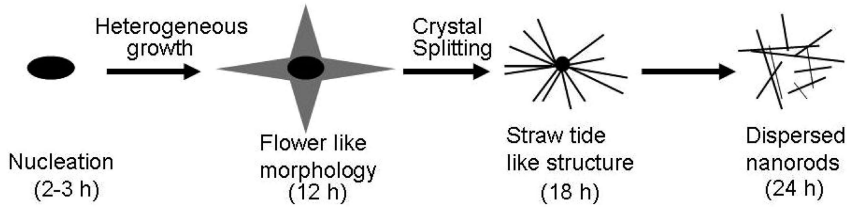

Figure 3. Schematic diagram, depicting possible morphology evolution of Sb_2S_3 from flowerlike morphology to nanorod through a straw tide like structure.

that are responsible for the cleavage of the crystal. Thus, the cleavage occurs parallel to the *c*-axis (00*l*), where only van der Waals bonds are ruptured. A similar phenomenon may be occurring in our case, and the petals of the flowerlike morphology split at the vulnerable sites, when subjected to suitable reaction conditions. The duration of the reaction appears to be the key factor accounting for the threshold energy required for these morphological transformations. This leads the crystal splitting, and gradually these nanorods are detached from the straw tide like structure resulting in well-dispersed nanorods. Earlier, Alivisatos et al. reported crystal splitting of Bi_2S_3 to form sheaflike or spherulite-type structures.[23] It is interesting to note that Sb_2S_3 has a similar type of crystal structure as that of the Bi_2S_3, which further ascertains our explanation for crystal splitting. More over, stibilite, a mineral of antimony, is also reported to exist in sheaflike structure, and it is believed by the mineralogist that this is due to the crystal splitting during growth of mineral.[24] The whole process of such morphological evolution has been described schematically as given in Figure 3.

The detailed structure and morphology of the sample has also been studied by TEM analysis and is presented in Figure 4. A low magnification image of a single nanorod with diameter around 150 nm is clearly seen in Figure 4a. In the inset is given the SAED pattern of the area marked on the nanorod. It consists of parallel aligned spot pattern indicating that the rods formed are single crystalline in nature. In Figure 4b is shown a HREM image of the nanorod, and the interlayer distance is found to be 0.364 nm which corresponds to the 101 plane of Sb_2S_3. The lattice planes are very well aligned in a parallel manner without

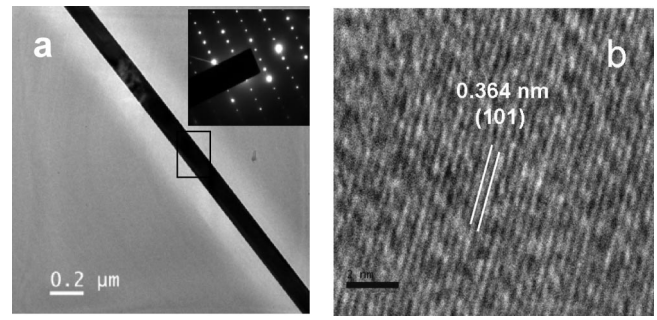

Figure 4. TEM images. (a) Low magnification image of part of a single nanorod, corresponding SAED (inset). (b) HREM image of the nanorod, demarcated plane corresponds to 101 plane.

any noticeable defects, which is very important from an optoelectronics application point of view.

To observe the effect of surfactant if any, the reaction has been carried out taking a neutral surfactant TX-100 instead of ionic SDS. It is observed that the reaction takes place in rather less time (12 h) and there could be seen some change in morphology of the final sample, though the product consists of mostly one-dimensional nanostructure only. The morphology has also been studied by SEM and TEM in this case and is presented in Figure 5. There could be observed one-dimensional nanostructures arranged into either bulky ball-like or straw tide like structure as depicted in Figure 5a. When one of these bulky balls is focused for obtaining more information about the product

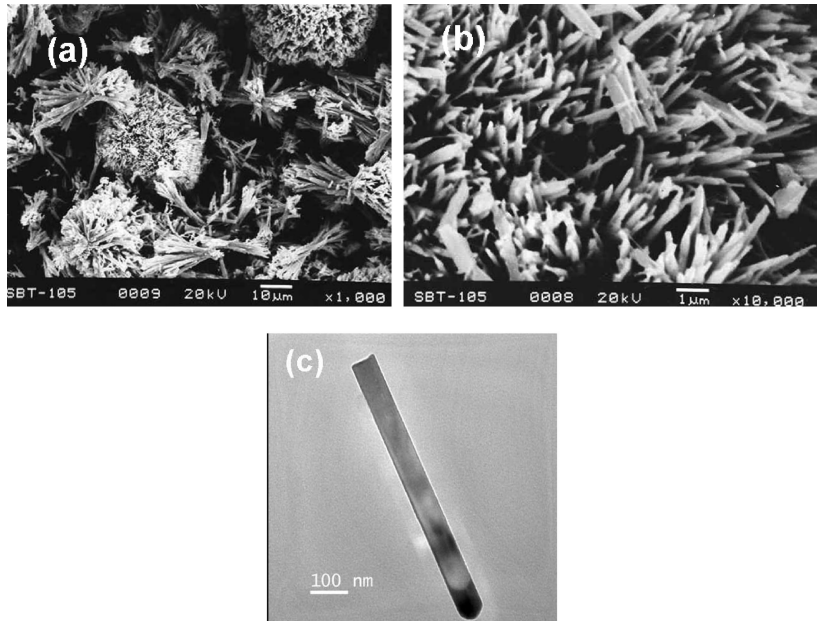

Figure 5. (a), (b) SEM image of the product obtained for 12 h of reaction when TX 100 is used as surfactant. (c) TEM micrograph of a single nanoflake.

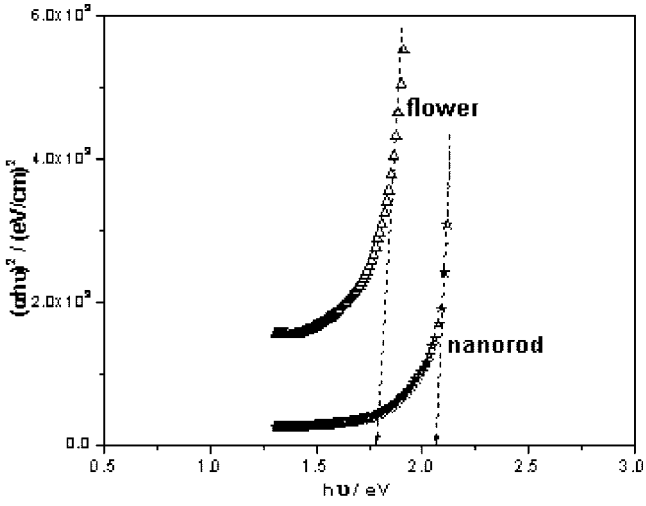

Figure 6. $(\alpha h\nu)^2$ versus $h\nu$ curve for the Sb_2S_3 flowerlike structure and nanorods.

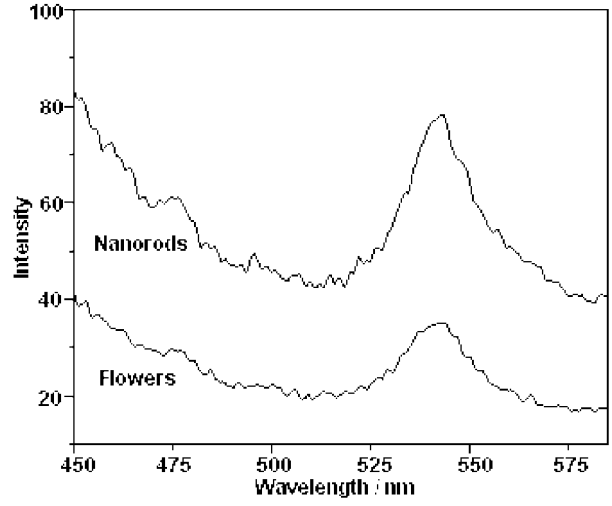

Figure 7. Photoluminescence spectra of the nanorod and flowerlike structures.

(Figure 5b), the tip of the nanostrcuctures is found to be rather flatter than the cylinder-like structures. Hence, it can be predicted that the 1D nanostructures are nanoflakes and not nanorods. Figure 5c represents a TEM micrograph of a single nanoflake with width around 80 nm and length 1 μm.

Sb_2S_3 is a very important material from the optoelectronics point of view due to its comparatively higher band gap among the other semiconductors of the same group. Hence, the optical properties of the nanorods as well as the flowerlike structures have been evaluated by means of optical absorption spectroscopy. The plots of $(\alpha h\nu)^2$ with respect to $h\nu$ of the samples are shown in Figure 6. It can be noted that the absorption below the threshold is higher in flowers than nanorods of Sb_2S_3. This may be due to the difference in morphology of the products obtained in both cases, and it has been reported earlier in the case of CdS thin films that the rough surface morphology reduces the transmission.[25] In the present case, flowerlike structures possess a rough surface morphology, which is responsible for reduced transmission and thereby its higher absorption in comparison to nanorods. Extrapolating the linear part of the curves on the $h\nu$ axis the band gap of the nanorods is found to be 2.08 eV and that of the flowerlike morphology is found to be 1.80 eV. The band gap observed in both cases is higher than that of the bulk value reported. However, band gap in the case of the nanorods is higher in comparison to the flowerlike morphology. It can be noted that the size of nanorods is bigger so that it excludes the possibility of quantum confinement effect. However, the low band gap of the flowers in comparison to the nanorods can be accounted on the basis of presence of impurity in the Fermi level in the case of flowerlike structures.

Luminescence spectroscopy is an equally important and a nondestructive tool for evaluating the optical nature of the materials. Photoluminescence spectra of both the products, recorded at excitation wavelength of 400 nm, are shown in Figure 7. It can be observed that both of the products have a peak at around 540 nm, but the peak intensity in the case of flowerlike morphology is comparatively lesser compared to that

of the nanorods. This could be due to two possible reasons: When the reaction was carried out for 12 h (resulting flower) there is a possibility of the presence of impurities resulting nonradiative recombination centers, where carriers are trapped resulting low intensity.[26] Moreover, crystallinity also plays a pivotal role in PL, where the intensity increases with improved crystal quality.[27] The nanorods obtained after duration of 24 h are supposed to be more crystalline than the flowerlike structures obtained after 12 h and consequently an increase in intensity. In addition, it has been reported that the shape of the material has a pronounced effect on the PL intensity, e.g. rodlike morphology has higher intensity than the sheetlike morphology.[28] In this case, the large surface area of the nanorods allows more electrons and holes to return to ground state via optically radiative recombination routes which increases the PL intensity. Hence, in our case, this may be one of the possible reasons for higher intensity of nanorods in comparison to flowerlike structure of Sb_2S_3. However, the PL spectra clearly suggest that Sb_2S_3 is a reasonably luminescent material and probably this property can be exploited for possible future applications.

Conclusion

To summarize the work described, nanorods of Sb_2S_3 have been synthesized by a surfactant assisted hydrothermal method. The formation of nanorods through flowerlike morphology with an intermediate straw tide like structure has been depicted by SEM study. This hierarchical transformation of novel structures to form nanorods as the final product is the first of its kind for this material. In the case of Sb_2S_3, there are also few reports of formation of novel structures based on systematic arrangement of nanorods as already discussed earlier. However, this is not another case of attachment or ordered arrangement of the nanorods to form novel structures; rather it is a reverse process, where nanorods are formed out of novel structures. A two-step heterogeneous nucleation−growth mechanism followed by crystal splitting has been described as the possible reason for this. The typical crystal structure of this material is responsible for the unusual crystal splitting. The band gaps of the products have been deduced from UV spectra, and that is found to be higher for Sb_2S_3 with nanorod than flower type morphology. Room temperature photoluminescence (PL) study suggests that nanorod of Sb_2S_3 is a reasonably luminescent material.

Acknowledgment. S.K.S. gratefully acknowledges DST and DRDO, India, for their financial supports to carry out this work. J.O. is thankful to CSIR, India.

References

(1) Li, M.; Schnablegger, H.; Mann, S. *Nature* **1999**, *402*, 393.
(2) Peng, X. G.; Manna, L.; Yang, W. D.; Wickham, J.; Scher, E.; Kadavanich, A.; Alivisatos, A. P. *Nature* **2000**, *404*, 59.
(3) Manna, L.; Scher, E. C.; Alivisatos, A. P. *J. Am. Chem. Soc.* **2000**, *122*, 12700.
(4) Kelly, N. E.; Lee, S.; Harris, K. D. M. *J. Am. Chem. Soc.* **2001**, *123*, 12682.
(5) Ball, P. *The Self-made tapestry: Pattern Formation in Nature*; Oxford University Press: Oxford, 1999.
(6) Zhao, S.; Roberg, H.; Yelon, A.; Veres, T. *J. Am. Chem. Soc.* **2006**, *128*, 12352.
(7) Liu, C.; Hu, Z.; Wu, Q.; Wang, X.; Chen, Y.; Sang, H.; Zhu, J.; Deng, S.; Xu, N. *J. Am. Chem. Soc.* **2004**, *127*, 1318.
(8) Shen, G. Z.; Chen, D.; Tang, K. B.; Li, F. Q.; Qian, Y. T. *Chem. Phys. Lett.* **2003**, *370*, 334.
(9) Datta, A.; Gorai, S.; Ganguli, D.; Choudhury, S. *Mater. Chem. Phys.* **2007**, *102*, 195.
(10) Cao, X.; Xie, Y.; Li, L. *J. Solid State Chem.* **2004**, *177*, 202.
(11) Hu, H.; Liu, Z.; Yang, B.; Mo, M.; Li, Q.; Yu, W.; Qian, Y. *J. Cryst. Growth* **2003**, *262*, 375.
(12) Mo, M.; Zhu, Z.; Yang, X.; Liu, X.; Zhang, S.; Gao, J.; Qian, Y. *J. Cryst. Growth* **2003**, *256*, 377.
(13) Cao, X.; Gu, L.; Wang, W.; Gao, W.; Zhuge, L.; Li, Y. *J. Cryst. Growth* **2006**, *286*, 96.
(14) Yu, Y.; Wang, R. H.; Chen, Q.; Peng, L. M. *J. Phys. Chem. B* **2005**, *109*, 23312.
(15) Wang, H.; Lu, N. Y.; Zhu, J. J.; Chen, H. Y. *Inorg. Chem.* **2003**, *42*, 6404.
(16) Ota, J. R.; Srivastava, S. K. *Cryst. Growth Des.* **2007**, *7*, 343.
(17) Yang, J.; Zeng, J. H.; Yu, S. H.; Yang, L.; Zhang, Y. H.; Qian, Y. T. *Chem. Mater.* **2000**, *12*, 2924.
(18) Hu, H.; Mo, M.; Yang, B.; Zhang, X.; Li, Q.; Yu, W.; Qian, Y. T. *J. Cryst. Growth* **2003**, *258*, 106.
(19) Lu, Q.; Zeng, H.; Wang, Z.; Cao, X.; Zhang, L. *Nanotechnology* **2006**, *17*, 2098.
(20) Juarez, B. H.; Rubio, S.; Dehesa, J. S.; Lopez, C. *Adv. Mater.* **2002**, *14*, 1486.
(21) El Idrissi Raghni, M. A.; Bonnet, B.; Hafid, M. L.; Fourcade, J. O.; Jumas, J. C. *J. Alloys Compd.* **1997**, *260*, 7.
(22) An, C.; Tang, K.; Yang, Q.; Qian, Y. *Inorg. Chem.* **2003**, *42*, 8081.
(23) Tang, J.; Alivisatos, A. P. *Nano Lett.* **2006**, *6*, 2701.
(24) Grigor'ev, D. P. *Antogeny of Minerals*; Israel Programme for Scientific Translations; Jerusalem, 1965.
(25) Zhang, H.; Ma, X.; Yang, D. *Mater. Lett.* **2003**, *58*, 5.
(26) Alvarado, J. L.; Lira, M. M.; Lopez, M. L. *Superficeas Vacio* **1997**, *7*, 51.
(27) Nazorov, M. V.; Kang, J. H.; Jeon, D. Y.; Popovici, E. J.; Muresan, L. B.; Tsukerblat, S. *Solid State Commun.* **2005**, *133*, 183.
(28) Wan, J.; Wang, Z.; Chen, X.; Li, M.; Qian, Y. *J. Cryst. Growth* **2005**, *284*, 538.

CG701133B